Proposed Mechanism and Functional Amino Acid Residues of Malonyl-CoA:Anthocyanin 5-*O*-Glucoside-6‴-*O*-Malonyltransferase from Flowers of *Salvia splendens*, a Member of the Versatile Plant Acyltransferase Family

Hirokazu Suzuki, Toru Nakayama,* and Tokuzo Nishino

Department of Biomolecular Engineering, Graduate School of Engineering, Tohoku University, Aoba-yama 07, Sendai, Miyagi 980-8579, Japan

Received October 7, 2002; Revised Manuscript Received November 25, 2002

ABSTRACT: The versatile plant acyltransferase (VPAT) family is a recently identified protein family consisting of acyltransferases involved in secondary metabolism in plants along with numerous homologues with as yet unidentified biochemical functions. Malonyl-CoA:anthocyanin 5-*O*-glucoside-6‴-*O*-malonyltransferase of *Salvia splendens* flowers (Ss5MaT1) is a member of this family that catalyzes the regiospecific transfer of the malonyl group from malonyl-CoA to the 6‴-hydroxyl group of the 5-glycosyl moiety of anthocyanins. To elucidate the mechanism and functional amino acid residues of VPAT family enzymes, steady-state kinetic analyses and site-directed mutagenesis of Ss5MaT1 guided by sequence comparison studies were carried out. On the basis of the results of product and dead-end inhibition studies as well as sequence comparison studies, the kinetic mechanism of Ss5MaT1 could be most consistently described in terms of a ternary complex mechanism in which both substrates and the enzyme form a complex before catalysis can occur, as in the case of chloramphenicol *O*-acetyltransferase (CAT) and histone acetyltransferase (HAT). Eight polar or ionizable amino acid residues that are invariant among 12 VPAT family enzymes were replaced by alanine, and the mutant enzymes were kinetically characterized. A significant diminution of the k_{cat} value was observed with the substitution of His167 (relative k_{cat}, 0.02%) and Asp390 (<0.01%), strongly suggesting that His167 and Asp390 are very important for catalytic activity. The log k_{cat} versus pH plots of the Ss5MaT1-catalyzed malonyl transfer suggested that a deprotonated active site group of p$K_a = 7.0 \pm 0.1$ may be involved in the catalytic steps of the "substrate to product" conversion in the ternary enzyme−substrate complex. Taking these lines of evidence together with the suggested similarity of the kinetic and catalytic mechanisms of Ss5MaT1 to those of CAT and HAT, the following Ss5MaT1 mechanism based on general acid/base catalysis was proposed: in the ternary complex, a general base deprotonates the 6‴-hydroxyl group of the anthocyanin substrate, thereby promoting a nucleophilic attack on the carbonyl of the thioester of malonyl-CoA; His167 and Asp390 appear to be involved in the general acid/base mechanism of Ss5MaT1.

Malonyl-CoA:anthocyanin 5-*O*-glucoside-6‴-*O*-malonyltransferase from scarlet sage (*Salvia splendens*) flowers (Ss5MaT1)[1] is an enzyme involved in the late stage of biosynthesis of salvianin [i.e., pelargonidin 3-*O*-(6″-*O*-caffeyl-*β*-glucopyranoside)-5-*O*-(4‴,6‴-*O*-dimalonyl-*β*-glucopyranoside)], a dimalonylated anthocyanin that predominantly occurs in *S. splendens* flowers (*1*). The enzyme specifically catalyzes the malonylation of the 6‴-hydroxyl group of the 5-glucoside moiety of anthocyanins, such as "bisdemalonylsalvianin" (Figure 1, compound **1a**) and shisonin (**1b**), to produce "monodemalonylsalvianin" (**2a**) and malonylshisonin (**2b**), respectively. We recently reported the purification to homogeneity, biochemical characterization, and gene cloning of Ss5MaT1, which revealed that the enzyme is a member of the versatile plant acyltransferase (VPAT) family (*1*). The VPAT family has been identified as an acyltransferase family (*2*) consisting of enzymes involved in secondary metabolism, including floral scent production (*3*) and anthocyanin biosynthesis (*1*, *4*−*6*), in plants. Although two highly conserved sequences [motifs 1 and 3 (Figure 2)] have been ubiquitously identified among members of the family, the entire amino acid sequences of the family members show only low similarities with each other (20−40% identity). It is likely that members of this family so far biochemically characterized represent only a small fraction of the total membership because *Arabidopsis* was recently estimated to contain about 70 related genes of the family, most of whose biochemical roles have yet to be determined (*7*).

To date, acyl-CoA-dependent acyltransferases have been shown to utilize one of two kinetically distinct mechanisms to catalyze acyl transfer, i.e., the double-displacement and the ternary complex mechanisms. For example, the acyl

* Corresponding author. Fax: +81-22-217-7293. E-mail: nakayama@seika.che.tohoku.ac.jp.

[1] Abbreviations: CAT, chloramphenicol *O*-acetyltransferase; CoA-SH, coenzyme A; HAT, histone acetyltransferase; Ss5MaT1, malonyl-CoA:anthocyanin 5-*O*-glucoside-6‴-*O*-malonyltransferase of *Salvia splendens*; VPAT, versatile plant acyltransferase.

10.1021/bi020618g CCC: $25.00
Published on Web 01/21/2003

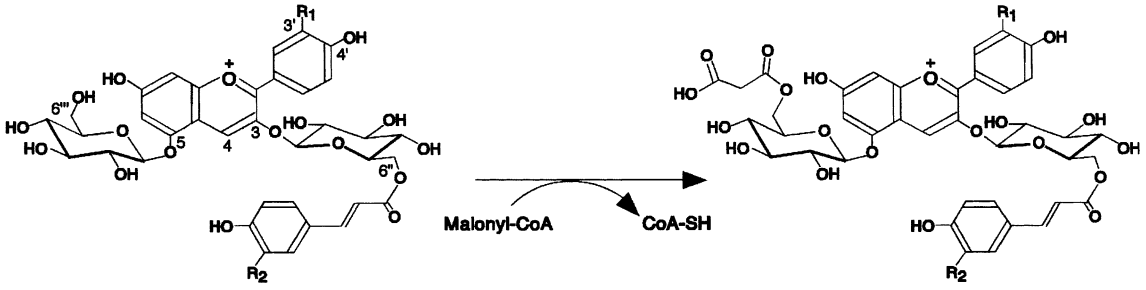

1 **2**

	R_1	R_2
1a, 2a	-H	-OH
1b, 2b	-OH	-H

FIGURE 1: Structures (in flavylium forms) of substrates, **1**, and products, **2**, of Ss5MaT1 with key positional numberings labeled on **1**. Ss5MaT1 malonylates bisdemalonylsalvianin (**1a**) to produce monodemalonylsalvianin (**2a**). Shisonin (**1b**) can also serve as a substrate for Ss5MaT1 to produce malonylshisonin (**2b**).

transfer catalyzed by thiolase [acetyl-CoA:acetyl-CoA *C*-acetyltransferases, EC 2.3.1.9 (*8*)] proceeds with a double-displacement mechanism that involves the acyl transfer from acyl-CoA to an enzyme nucleophile (a cysteine residue) prior to transfer to the second substrate (*8*). On the other hand, chloramphenicol *O*-acetyltransferase [CAT, EC 2.3.1.28 (*9*)] and histone acetyltransferase [HAT (*10*)] operate through ternary complex mechanisms, which require both substrates and the enzyme to form a ternary complex before direct acyl transfer from acyl-CoA to the substrate acceptor, without the formation of a covalent acyl-enzyme intermediate (*10*−*12*). The roles of the active site amino acid residues of these kinetically established acyltransferases have also been studied in detail in terms of their three-dimensional structures (*13*, *14*).

The VPAT family is functionally and phylogenetically distinct from the known acyl-CoA-dependent acyltransferases mentioned above, and their three-dimensional structures, kinetic and catalytic mechanisms, and identity, as well as the role(s) of active site residues, are not yet known. So far, the importance of the histidine residue in the catalytic functioning of the VPAT enzymes has only been implicated on the basis of the observation that many of the family enzymes are inactivated by diethyl pyrocarbonate (*1*, *2*, *5*). In addition, sequence comparison studies have suggested that VPAT enzymes might be mechanistically related to CAT (*2*). However, no experimental details on the basis of kinetic and mechanistic studies have been obtained to further address these issues.

Here, we report on the kinetic and site-directed mutagenesis studies of Ss5MaT1 undertaken to probe the mechanism and functional amino acid residues of VPAT family enzymes. In the absence of three-dimensional structural information on the family, intensive sequence comparison among members of this family permits the selection of targets for alanine-scanning mutagenesis studies to identify functional amino acid residues. These results, combined with those of the steady-state kinetic studies, allowed us to propose the mechanism of the acyl transfer catalyzed by VPAT family enzymes.

EXPERIMENTAL PROCEDURES

Materials. Shisonin [cyanidin 3-*O*-(6″-*O*-*p*-coumarylglucoside)-5-*O*-glucoside; Figure 1, compound **1b**] and malonylshisonin [cyanidin 3-*O*-(6″-*O*-*p*-coumarylglucoside)-5-*O*-(6‴-*O*-malonylglucoside), **2b**] were purified as described previously, and their structures were confirmed by 500 MHz ^{1}H and ^{13}C NMR as well as by MS analyses (*1*). Malonyl-CoA and coenzyme A (CoA-SH) were purchased from Nacalai Tesque, Kyoto, Japan. All other chemicals were of the highest grade commercially available.

Ss5MaT1 Assay. The standard assay mixture (final volume, 100 μL) consisted of 20 mM potassium phosphate (pH 7.0), 120 μM shisonin, 60 μM malonyl-CoA (final concentrations), and the enzyme. The mixture without enzyme was preincubated at 30 °C, and the reaction was started by enzyme addition. After incubation at 30 °C for 10−20 min, the reaction was stopped by adding 200 μL of ice-cold 0.5% (by volume) trifluoroacetic acid. Anthocyanins in the reaction mixture were analyzed by reversed-phase HPLC on a Shodex Asahipak ODP-50 4E column (4.6 mm × 250 mm; Showa Denko, Tokyo) as described previously (*1*). Kinetic parameters and their standard errors were estimated from the initial velocity data by nonlinear regression analysis (*15*). The pH dependence of kinetic parameters was determined as described above except that the concentration of the phosphate buffer was set at 0.1 M (final concentration), and the pH was varied from 5.0 to 8.5; the buffering capacity was sufficient for present enzyme assays. The determination of the kinetic parameters at pHs higher than 8.6 was difficult because of the instability of the enzyme (*1*). The pH profiles [log k_{cat} versus pH and log(k_{cat}/K_m) versus pH] were fitted as described by Cleland (*16*) and Copeland (*17*) using the two-dimensional scientific graph-plotting-tool program and least-squares analysis. Protein was determined by the method of Bradford (*18*) using a kit (Bio-Rad, Hercules, CA) with bovine serum albumin as the standard.

Product Inhibition Studies. Inhibition by CoA-SH and by malonylshisonin, the product inhibitors, was kinetically analyzed under steady-state conditions using the standard

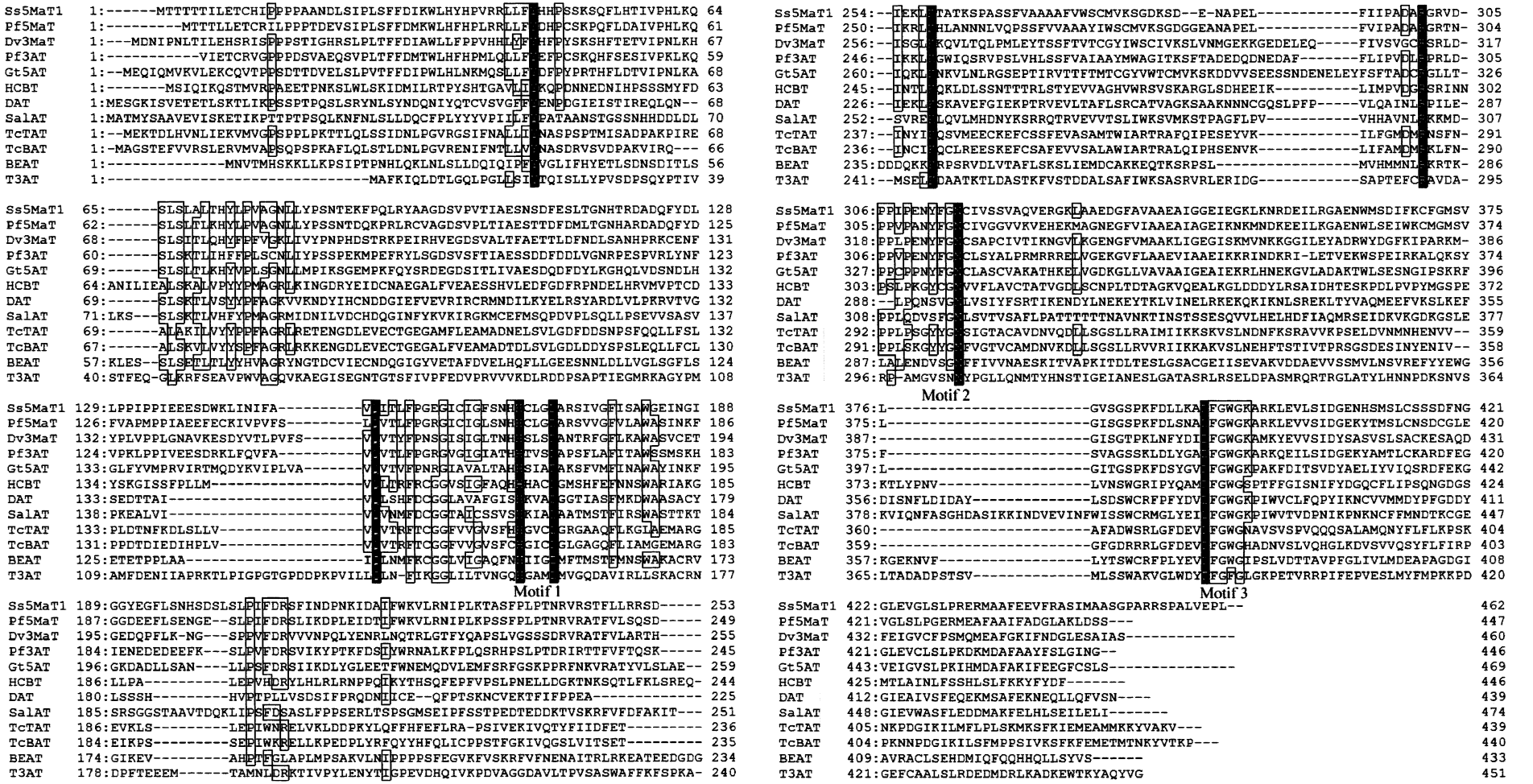

FIGURE 2: Multiple alignment of deduced amino acid sequences of the VPAT family enzymes. Boxes indicate that more than six out of 12 sequences have been conserved. Locations of motifs 1, 2, and 3 are indicated below the sequences. Invariant residues in the Ss5MaT1 sequence are shown in white type on a black background and are the sites of substitution by alanine. The enzymes used for alignment were as follows: Ss5MaT1 [GenBank accession number AF405707 (*1*; this study)]; Pf5MaT, malonyl-CoA:anthocyanin 5-*O*-glucoside-6‴-*O*-malonyltransferase of *Perilla frutescens* (AF405204); Dv3MaT, malonyl-CoA:anthocyanin 3-*O*-glucoside-6″-*O*-malonyltransferase of *Dahlia variabilis* [AF489108 (*6*)]; Pf3AT, hydroxycinnamoyl-CoA:anthocyanin 3-*O*-glucoside-6″-*O*-acyltransferase of *P. frutescens* [BAA93475 (*5*)]; Gt5AT, hydroxycinnamoyl-CoA:anthocyanin 5-*O*-glucoside-6″-*O*-acyltransferase of *Gentiana triflora* [BAA74428 (*4*)]; HCBT, hydroxycinnamoyl/benzoyl-CoA:anthranilate *N*-hydroxycinnamoyl/benzoyltransferase of *Dianthus caryophyllus* L. [CAB06430 (*26*)]; DAT, deacetylvindoline 4-*O*-acetyltransferase from *Catharanthus roseus* [AAC99311 (*10*)]; SalAT, salutaridinol 7-*O*-acetyltransferase of *Papaver somniferum* [AAK73661 (*27*)]; TcTAT, taxadienol acetyltransferase of *Taxus cuspidata* [AAF34254 (*28*)]; TcBAT, 10-deacetylbaccatin III 10-*O*-acetyltransferase of *T. cuspidata* [AAF27621 (*29*)]; BEAT, acetyl CoA:benzylalcohol acetyltransferase from *Clarkia breweri* [AAC18062 (*3*)]; T3AT, trichothecene 3-*O*-acetyltransferase of *Fusarium graminearum* [BAA24430 (*30*)].

Table 1: Primers Used for Site-Directed Alanine Mutagenesis of Ss5MaT1

enzyme	DNA sequence[a,b]
Y45A	5′-CGCCGCCTCCTCTTCGCCCACCACCCTTCCTCC-3′
Q150A	5′-CAACATTTTCGCGGTTGCGATCACTCTGTTCCCC-3′
H167A[c]	5′-GGCGTCGCCGAGGCAGGCGTGATTGGAGAAACC-3′
D171A	5′-CACCACTGCCTCGGCGCCGCCAGATCTATCGTCGG-3′
K258A[c]	5′-GGCGATTTAGTGGCGGTTGCCAGCTTCTCGATGTCGG-3′
R301A	5′-CATACCTGCGGACGCCGCGGGGAGGGTGGACCCG-3′
N315A	5′-GGAAAATTACTTCGGCGCCTGCATCGTGAGC-3′
D390A	5′-CGATCTGTTGAAGGCGGCTTTTGGATGGGGAAAGG-3′
selection 1	5′-GCATGCGAGCTC*GGTTCC*CCGGGTCGACCTGC-3′
selection 2[c]	5′-GCAGGTCGACCC*GGGGAACC*GAGCTCGCATGC-3′

[a] The underlined bases indicate the positions that were changed. [b] The underlined and italicized bases indicate the *Kpn*I deletion site in the multicloning site. [c] The primers were designed antisense for Ss5MaT1 cDNA.

assay system (see above) with varying concentrations of malonyl-CoA and shisonin. To determine whether inhibition was competitive (eq 1), uncompetitive (eq 2), or noncompetitive (eq 3), the data were fitted to the respective inhibition equations using the two-dimensional scientific graph-plotting-tool program and least-squares analysis.

$$1/v = 1 / V + K_m\{1 + ([I]/K_i)\}/V[S] \quad (1)$$

$$1/v = \{1 + ([I]/K_i)\}/V + K_m/V[S] \quad (2)$$

$$1/v = \{1 + ([I]/K_i')\}/V + K_s\{1 + ([I]/K_i)\}/V[S] \quad (3)$$

Site-Directed Mutagenesis and Expression. In vitro mutagenesis was carried out using a Chameleon double-stranded, site-mutagenesis kit (Stratagene, La Jolla, CA) and the plasmid pSs5MaT1 (*1*) as a template according to the manufacturer's guidelines to obtain the following site-directed mutants of Ss5MaT1, Y45A, Q150A, H167A, D171A, K258A, R301A, N315A, and D390A, which represent Ss5MaT1 mutants with a replacement by alanine of Tyr45, Gln150, His167, Asp171, Lys258, Arg301, Asn315, and Asp390, respectively (see also Figure 2 for mutation sites). Briefly, the plasmid pSs5MaT1 was heat-denatured, and two oligonucleotide primers, i.e., selection and mutagenic primers, were simultaneously annealed to one of the strands of the plasmid. The sequences of the mutagenic and selection primers are shown in Table 1. The selection primers were also designed to inactivate a *Kpn*I site in the multicloning site of pSs5MaT1. Both of the annealed primers were extended around the plasmid using T7 DNA polymerase and T4 DNA ligase. The resultant DNA mixture was then treated with *Kpn*I; mutant plasmids remained undigested, whereas the parental plasmids were digested. The mixture was then used to transform *Escherichia coli* strain XL*mutS* cells (Stratagene) having a repair-deficient phenotype. The transformants were grown in an LB medium containing 50 μg/mL ampicillin. Plasmid DNA was isolated from the cells and digested with a restriction enzyme (*Kpn*I) corresponding to the selection primer. Epicurian Coli XL-1 Blue cells (Stratagene) were then transformed with the resultant DNA digest and grown to amplify the plasmid encoding the mutated *Ss5MaT1* gene. Individual mutations were verified by DNA sequencing using a dye-terminater cycle sequencing kit (Beckman Coulter) with a CEQ 2000 DNA analysis system (Beckman Coulter, Fullerton, CA). The GENETYX program (Software Development, Tokyo) was used for computer analysis of the nucleotide and deduced amino acid sequences.

The wild-type and mutant Ss5MaT1 were expressed as an in-frame N-terminal fusion with a His_6 tag in *E. coli* JM109 transformant cells, as described (*1*). The expressed proteins were purified to apparent homogeneity, as judged by sodium dodecyl sulfate−polyacrylamide gel electrophoresis analysis (*19*) from crude extracts of the transformant cells, as described previously (*1*).

RESULTS

Kinetic Mechanism. Ss5MaT1-catalyzed malonyl transfer to anthocyanin (Figure 1) is a Bi-Bi system, according to Cleland's nomenclature (*20*, *21*), and there are two possible kinetic mechanisms for the system: a double-displacement or a ternary complex. We previously showed that *p*-coumaric acid, which mimics the aromatic acyl portion of an anthocyanin substrate, can serve as a dead-end inhibitor of Ss5MaT1; it was an uncompetitive inhibitor with respect to malonyl-CoA and a competitive one with respect to shisonin (*1*). These types of dead-end inhibition suggest a ternary complex mechanism of Ss5MaT1-catalyzed malonyl transfer to anthocyanin. To further confirm the formation of the ternary complex during Ss5MaT1-catalyzed malonyl transfer, product inhibitions were studied.

Initial velocities were determined with CoA-SH as a product inhibitor, and the data were plotted in double-reciprocal form for $1/v$ versus 1/[malonyl-CoA] and $1/v$ versus 1/[shisonin] at several fixed inhibitor concentrations (Figure 3). In the case of $1/v$ versus 1/[malonyl-CoA], a series of lines intersecting on the $1/v$ axis were obtained (Figure 3A), indicating competitive inhibition by CoA-SH toward the malonyl-CoA substrate. The $1/v$ versus 1/[shisonin] plots gave a series of straight lines intersecting in the second quadrant (Figure 3B), indicative of noncompetitive inhibition by CoA-SH toward the shisonin substrate. When malonylshisonin was used as a product inhibitor, it acted as a noncompetitive inhibitor toward both the malonyl-CoA (Figure 3C) and shisonin (Figure 3D). These results corroborated that the Ss5MaT1 reaction involves the formation of a ternary complex, the [malonyl-CoA−anthocyanin−enzyme] complex, prior to chemical catalysis. It should be mentioned that, if the Ss5MaT1-catalyzed acyl transfer proceeds with a double-displacement mechanism, the $1/v$ versus 1/[malonyl-CoA] plots (Figure 3A) should show a noncompetitive inhibition by CoA-SH toward the malonyl-CoA substrate, and the $1/v$ versus 1/[shisonin] plots (Figure 3B) should show a competitive inhibition by CoA-SH toward the shisonin substrate.

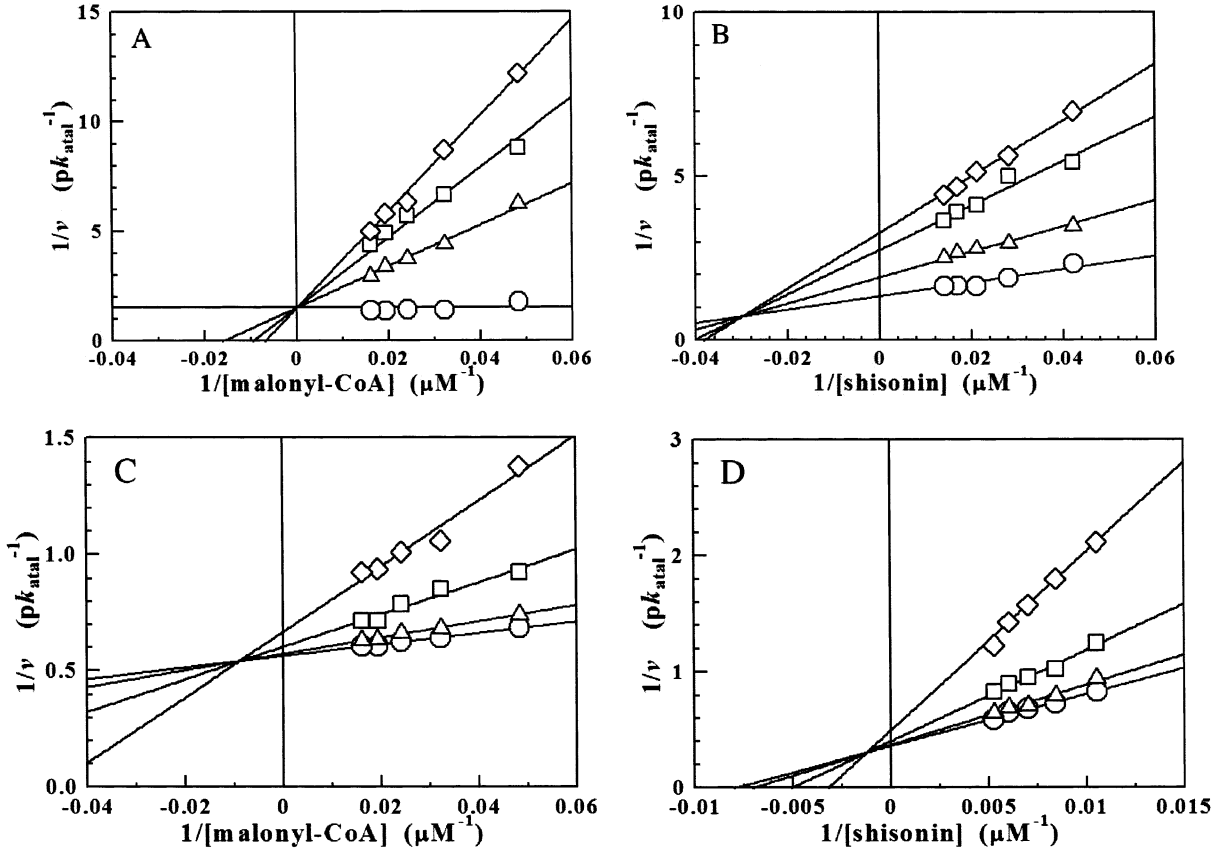

FIGURE 3: Kinetic analysis of product inhibition of Ss5MaT1-catalyzed malonyl transfer. The data are presented in double-reciprocal form. (A) Competitive inhibition by CoA-SH toward malonyl-CoA. $1/v$ is plotted versus 1/[malonyl-CoA] at a fixed concentration (71 μM) of shisonin and several fixed concentrations of CoA-SH (circles, 0 mM; triangles, 0.5 mM; squares, 0.75 mM; diamonds, 1.0 mM). The malonyl-CoA concentrations spanned 21−62 μM. (B) Noncompetitive inhibition by CoA-SH toward shisonin. $1/v$ is plotted versus 1/[shisonin] at a fixed concentration (62 μM) of malonyl-CoA and several fixed concentrations of CoA-SH (circles, 0 mM; triangles, 0.25 mM; squares, 0.5 mM; diamonds, 0.75 mM). The shisonin concentrations spanned 24−71 μM. (C) Noncompetitive inhibition by malonylshisonin toward malonyl-CoA. $1/v$ is plotted versus 1/[malonyl-CoA] at a fixed concentration (95 μM) of shisonin and several fixed concentrations of malonylshisonin (circles, 0 μM; triangles, 3 μM; squares, 6 μM; diamonds, 12 μM). The malonyl-CoA concentrations spanned 21−62 μM. (D) Noncompetitive inhibition by malonylshisonin toward shisonin. $1/v$ is plotted versus 1/[shisonin] at a fixed concentration (41 μM) of malonyl-CoA and several fixed concentrations of malonylshisonin (circles, 0 μM; triangles, 3 μM; squares, 6 μM; diamonds, 9 μM). The shisonin concentrations spanned 95−190 μM.

Effects of pH on Kinetic Parameters. The kinetic parameters of Ss5MaT1-catalyzed malonyl transfer to shisonin were determined over a pH range of 5.0 to 8.5 (Figure 4), at which the enzyme stability is maintained under the assay conditions (*1*). In the pH range employed, the pH dependence of the $\log(k_{cat}/K_m)$ value for shisonin showed a profile with slope = 1 that subsequently leveled off at high pHs with an apparent pK_a of 6.6 ± 0.1 (Figure 4A). For comparison, the absorption spectra of the substrate shisonin were also pH-dependent in the pH range of 5.0−9.0 (not shown) and showed a pK_a value of 7.3 ± 0.1, representing an interconversion of the aglycon part of the substrate between the species absorbing at 530 nm (pH <7.3; assigned as the neutral quinonoidal base isomers)[2] and that absorbing at 593 nm (pH >7.3; assigned as the anionic quinonoidal base isomers) (H. Suzuki, T. Nakayama, and T. Nishino, unpublished results); however, the k_{cat}/K_m value for shisonin was essentially independent of the pH in the range of 7−8 (Figure 4A), suggesting the involvement of a deprotonated group of pK_a = 6.6 ± 0.1 in shisonin binding and/or catalysis. The k_{cat}/K_m value for malonyl-CoA showed only a small variation in the pH range employed here (Figure 4B), though its maximum was found at pH 6.7. The log k_{cat} versus pH profile displayed a bell-shaped profile with two pK_a values, one of which was determined to be 7.0 ± 0.1 and was of critical importance for catalysis (Figure 4C).

Sequence Alignment-Guided Alanine-Scanning Mutagenesis Studies. In an attempt to identify functional amino acid residues of Ss5MaT1 by site-directed mutagenesis, we then undertook an alanine-scanning mutagenic program targeting the key active site residues in Ss5MaT1 using predictions from a comparative sequence analysis. The sequences of 12 VPAT family enzymes from diverse sources were compared (Figure 2). Polar or ionizable amino acid residues that are fully conserved among these sequences were selected as targets for alanine-scanning mutagenesis. Eight invariant

[2] The pH-dependent transformation of the structure of anthocyanidins, i.e., the aglycon part of substrate anthocyanins, is proposed as follows (*22*). At acidic pHs (pH <2), anthocyanin is present in its cationic flavylium form, which is red in color. At pHs of 5−7, the neutral 7- and 4-quinonoidal base isomers (bluish purple in color) are produced from the flavylium cation through prototropic tautomerism, which subsequently results in the production of the anionic 7- and 4-quinonoidal base isomers (blue in color) at pHs higher than 7, which are dependent on anthocyanins. At pHs higher than 5, the anthocyanins also slowly undergo hydration to produce a colorless carbinol pseudobase species. However, the formation of the colorless carbinol pseudobase species of substrate and product should be negligible under the assay conditions, considering the spectral stability of these anthocyanins (see ref *6* for details).

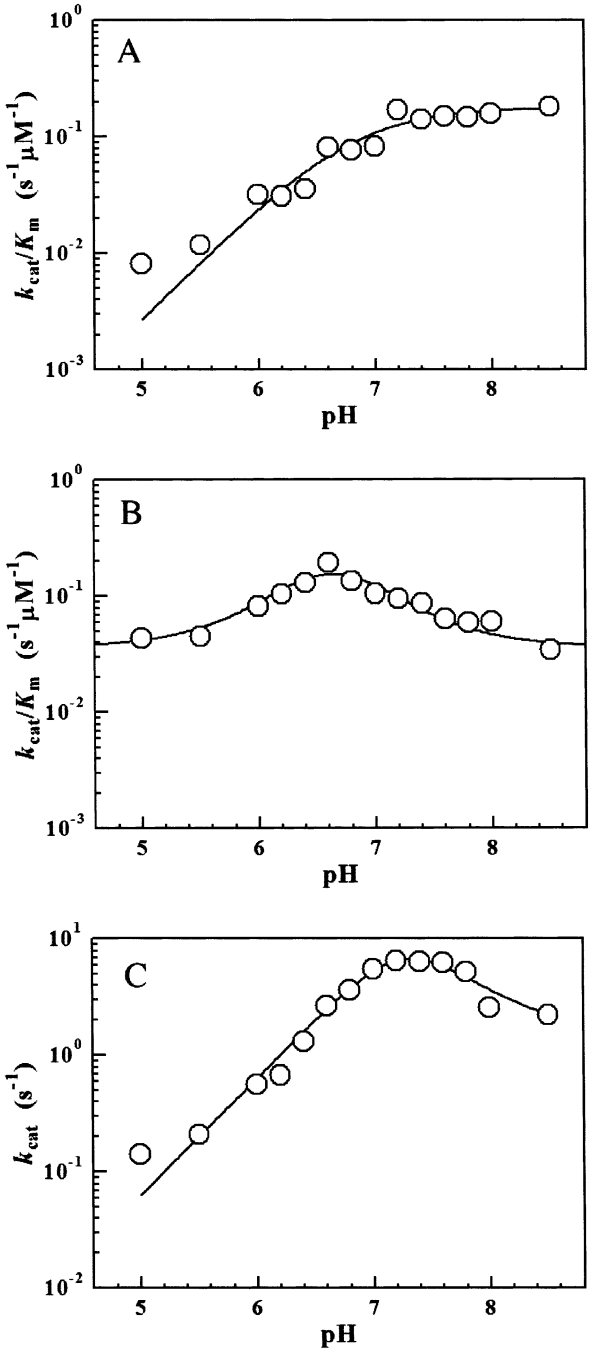

FIGURE 4: Effects of pH on k_{cat}/K_m for shisonin (A), k_{cat}/K_m for malonyl-CoA (B), and k_{cat} (C) of Ss5MaT1-catalyzed malonyl transfer to shisonin. Experimental conditions were as described under Experimental Procedures. Standard errors of kinetic data were within ±20%, except that those of the k_{cat}/K_m value for shisonin at pH 5.0 and of the k_{cat} value at pH 5.0 were within ±56%.

polar or ionizable residues (Tyr45, Gln150, His167, Asp171, Lys258, Arg301, Asn315, and Asp390) were identified, three of which (His167, Asp171, and Asp390) are located in motifs 1 and 3, which are invariant among the members of this family (*1*, *4*−*6*). These eight residues were replaced by alanine to probe their roles in catalysis. The kinetic properties of these eight mutants were analyzed; the results are summarized in Table 2. A significant loss of k_{cat} was observed when alanine was substituted for His167 (present in motif 1; relative k_{cat}, 0.02%) and Asp390 (in motif 3; relative k_{cat}, <0.01%) (Table 2). Because the functional importance of the histidine residue has been indicated from previous studies with several enzymes of this family, we further examined the effect of substitution by alanine of His166 and Cys168, both of which juxtapose His167 and are well conserved among several members of the family, to confirm the specific importance of His167 for catalytic functioning among these three, contiguous, well-conserved residues (Figure 2). The results showed that these substitutions did not cause any significant inactivation [relative activities under standard assay conditions (see Experimental Procedures): wild-type, 100%; H166A, 23%; C168A, 8%]. A relatively large loss of k_{cat} was also observed with replacement by alanine of Asp171 (in motif 1; 125-fold diminution) and Asn315 (in motif 2; 91-fold diminution).

DISCUSSION

The results obtained from steady-state kinetic analyses of Ss5MaT1 inhibitions by product and dead-end inhibitors were consistent with the ternary complex mechanism of Ss5MaT1-catalyzed malonyl transfer. This was also corroborated by the results of the present sequence comparison studies, as follows. Acyl-CoA-dependent acyl transfer through the double-displacement mechanism is exemplified by thiolase catalysis (*8*), in which a thioester intermediate between the acyl group and enzyme nucleophile (a cysteine residue) is transiently formed prior to the acyl transfer. If Ss5MaT1 operates with the same kind of mechanism as thiolase, an invariant cysteine (or serine) residue participating in thioester (or ester) linkage formation has to exist in the sequence of each VPAT family enzyme, given the employment of a common reaction mechanism by members of the same enzyme family. However, multiple sequence alignment of the VPAT family enzymes did not show the invariant conservation of these residues (Figure 2). Therefore, a serine- or cysteine-mediated double-displacement mechanism for the Ss5MaT1 catalysis is highly unlikely. Taking these lines of evidence together, we propose that SsMaT1-catalyzed malonyl transfer proceeds with the formation of a ternary complex, as in the cases of CAT and HAT catalysis (*10*, *11*). Moreover, the Ss5MaT1-catalyzed acyl transfer can be consistently explained in terms of the ordered Bi-Bi mechanism on the basis of the product inhibition results (i.e., one competitive and three noncompetitive inhibition patterns). Because CoA-SH was a competitive inhibitor with respect to malonyl-CoA (Figure 4A), malonyl-CoA was the first substrate to bind to the enzyme and CoA-SH was the last product to dissociate from the enzyme−product complex. This compulsory order of binding of substrates was consistent with the uncompetitive inhibition pattern by *p*-coumaric acid with respect to malonyl-CoA as reported previously (*1*).

To date, the reaction mechanisms and catalytic residues of CAT and HAT have been extensively studied in relation to three-dimensional enzyme structures (*13*, *14*, *23*, *24*). These enzymes have been shown to share common mechanistic features of acyl transfer: in the ternary complex, a general base activates the nucleophilic group of the acyl acceptor by deprotonation, promoting its nucleophilic attack on the carbonyl carbon of the acyl-CoA. In CAT and HAT, His195 and Glu173 have respectively been proposed to fulfill the role of a general base during catalysis: the His195 of CAT deprotonates a hydroxyl group of chloramphenicol (*23*) and the Glu173 of HAT deprotonates an ϵ-amino group of a specific lysine residue of the substrate histone (*24*).

Table 2: Kinetic Parameters of Selected Ss5MaT1 Mutants[a]

		shisonin		malonyl-CoA	
mutant[b]	k_{cat} (s^{-1})	K_m (μM)	k_{cat}/K_m (s^{-1} μM^{-1})	K_m (μM)	k_{cat}/K_m (s^{-1} μM^{-1})
wild type	8.7 ± 0.5 (100)	35 ± 5	0.25 (100)	22 ± 3	0.40 (100)
Y45A	1.0 ± 0.1 (11)	19 ± 3	0.053 (21)	13 ± 1	0.08 (20)
Q150A	5.8 ± 0.3 (67)	39 ± 5	0.15 (60)	14 ± 2	0.41 (103)
H167A	0.002 ± 0.001 (0.02)	5.4 ± 2.8	0.00037 (0.2)	6.4 ± 1.8	0.0003 (0.1)
D171A	0.072 ± 0.013 (0.8)	490 ± 100	0.00015 (0.1)	71 ± 27	0.001 (0.3)
K258A	5.3 ± 0.3 (61)	44 ± 5	0.12 (48)	20 ± 2	0.27 (68)
R301A	1.4 ± 0.1 (17)	84 ± 10	0.017 (7)	35 ± 4	0.04 (10)
N315A	0.10 ± 0.01 (1.1)	62 ± 8	0.0016 (0.6)	25 ± 5	0.004 (1)
D390A	<0.001 (<0.01)				

[a] Values in parentheses indicate the relative percent of the k_{cat} and k_{cat}/K_m values of mutants, with those of the wild-type enzyme taken to be 100%. [b] Polar or ionizable amino acid residues that are fully conserved among the members of the family (see Figure 2) were selected as targets for alanine-scanning mutagenesis. For the nomenclature of mutants, see Experimental Procedures.

Scheme 1: Proposed Catalytic Mechanism of Ss5MaT1[a]

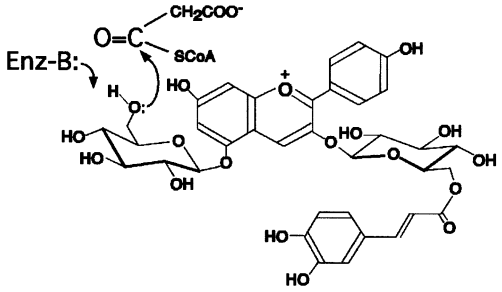

[a] His167 (or Asp390) may act as a general base (Enz-B:) during catalysis. For the sake of convenience, the aglycon part of the malonyl acceptor is shown in its flavylium form.

Because, as we have shown, the kinetic mechanism of Ss5MaT1-catalyzed malonyl transfer also appears to agree with the ternary complex mechanism, the Ss5MaT1 catalytic mechanism should also share such common features with the CAT and HAT mechanisms. Thus, in the ternary [malonyl-CoA−anthocyanin−Ss5MaT1] complex, a general base would deprotonate the 6‴-hydroxyl of the acyl acceptor to facilitate its nucleophilic attack on the carbonyl carbon of acyl-CoA (Scheme 1).

To probe functional amino acid residues involved in the Ss5MaT1 mechanism on the basis of the general acid/base catalysis proposed above, alanine-scanning mutagenesis guided by sequence comparison, as well as pH-dependent kinetic studies, was carried out. The mutagenesis studies revealed that a 5000−10000-fold diminution in k_{cat} value was accompanied by the substitution by alanine of two invariant residues: His167 and Asp390 (Table 2). This strongly suggests that these residues may be related to the role as a general base in the ternary "enzyme−substrate" complex. Although the functional importance of the histidine residue (in motif 1) has been implicated from previous sequence comparisons and chemical modification results, the crucial importance of the aspartic acid residue (in motif 3) for the catalytic activity of the VPAT family enzymes has been, for the first time, identified in the present studies. The k_{cat} versus pH plots of the Ss5MaT1-catalyzed malonyl transfer suggested that a deprotonated active site group of $pK_a = 7.0 \pm 0.1$ may be involved in the catalytic steps of the chemical conversion in the ternary enzyme−substrate complex. Although the pK_a value of 7.0 ± 0.1 likely reflects the ionization of the histidine residue (*1*, *2*, *5*), to which His167 could be assigned, it is also possible that this value represents the ionization of a perturbed carboxylic acid residue (i.e., aspartic acid or glutamic acid residue; e.g., Asp390) or that of some other residue within the specialized environment of the complex (*17*, *23*). However, considering the fact that there are many examples of enzyme mechanisms, such as those of serine proteinases, α/β hydrolases, and CAT (see above), which utilize a histidine residue as a general base to deprotonate the primary alcoholic hydroxyl group to enhance the nucleophilicity of the hydroxyl oxygen, we prefer His167 as the most likely candidate for the general base involved in the Ss5MaT1 mechanism. Moreover, it is tempting to speculate that, in the Ss5MaT1 mechanism, there may be a "carboxylate−imidazole (His167)−hydroxyl (substrate)" relay system, which is analogous to the catalytic triads of serine proteinases and α/β hydrolases, as the machinery to enhance the nucleophilicity of the hydroxyl group of substrate anthocyanin: Asp390 could be a carboxylate member of such a system. Three-dimensional structural information on Ss5MaT1 is necessary to address these issues. It is worth noting that the invariant His-Xaa_3-Asp sequence, which is reminiscent of motif 1 of VPAT family enzymes, has also been identified among CAT sequences of a variety of origins (*1*, *2*), and the functional importance of this sequence in the catalytic mechanism of *E. coli* CAT has been demonstrated. Namely, His195 at the first position of this conserved sequence of CAT is proposed to serve as the general base that abstracts the hydroxyl group of chloramphenicol during catalysis, whereas Asp199 at the fifth position is important for maintaining proper orientation of active site residues for catalytic activity through its salt bridge formation (*13*). Considering the observed large loss of the k_{cat} and $k_{cat}/K_{m,shisonin}$ values upon D171A substitution of Ss5MaT1, it is likely that Asp171 of Ss5MaT1 is located at or near the active site and plays an important role (either direct or indirect) for catalytic activity. A large loss of the enzyme activity was also observed with N315A substitution. Because Asn315 is located in motif 2, which is specifically identified with anthocyanin acyltransferases, we initially assumed that this observation might arise from the loss of the enzyme's ability to bind substrate anthocyanins upon the N315A substitution. Unexpectedly, however, the N315A substitution exclusively diminished the k_{cat} value of the enzyme and did not essentially affect K_m values for shisonin and malonyl-CoA. These results suggest that Asn315 is also located at or near the active site and plays an important role for catalytic action of this enzyme. Replacement of other invariant residues (Tyr45, Gln150, Lys258, and Arg301) by

alanine caused no significant diminution in the kinetic parameters, and these residues are, probably, not directly involved in primary catalysis.

In conclusion, on the basis of the results presented above, the following general mechanism for acyl transfer catalyzed by VPAT family enzymes is proposed. Acyl transfer catalyzed by VPAT family enzymes most likely proceeds under a ternary complex mechanism involving the enzyme, acyl-CoA, and an acyl acceptor. Once the ternary complex has formed, a general base in the complex promotes the nucleophilic attack of the acyl acceptor on the carbonyl carbon of acyl-CoA. Histidine (in motif 1) and aspartic acid (in motif 3) residues should be involved in the general acid/base mechanism of VPAT catalysis.

ACKNOWLEDGMENT

We are grateful to Dr. Yoshikazu Tanaka, Suntory Ltd., for participation in valuable discussions. We are also indebted to Prof. Masa-atsu Yamaguchi, Minami-Kyushu University, for providing substrate anthocyanins.

REFERENCES

1. Suzuki, H., Nakayama, T., Yonekura-Sakakibara, K., Fukui, Y., Nakamura, N., Nakao, M., Tanaka, Y., Yamaguchi, M., Kusumi, T., and Nishino, T. (2001) *J. Biol. Chem. 276*, 49013−49019.
2. St-Pierre, B., Laflamme, P., Alarco, A.-M., and De Luca, V. (1998) *Plant J. 14*, 703−713.
3. Dudareva, N., D'Auria, J. C., Nam, K. H., Raguso, R. A., and Pichersky, E. (1998) *Plant J. 14*, 297−304.
4. Fujiwara, H., Tanaka, Y., Yonekura-Sakakibara, K., Fukuchi-Mizutani, M., Nakao, M., Fukui, Y., Yamaguchi, M., Ashikari, T., and Kusumi, T. (1998) *Plant J. 16*, 421−431.
5. Yonekura-Sakakibara, K., Tanaka, Y., Fukuchi-Mizutani, M., Fujiwara, H., Fukui, Y., Ashikari, T., Murakami, Y., Yamaguchi, M., and Kusumi, T. (2000) *Plant Cell Physiol. 41*, 495−502.
6. Suzuki, H., Nakayama, T., Yonekura-Sakakibara, K., Fukui, Y., Nakamura, N., Yamaguchi, M.-A., Tanaka, Y., Kusumi, T., and Nishino, T. (2002) *Plant Physiol. 130*, 2142−2151.
7. Dudareva, N., and Pichersky, E. (2000) *Plant Physiol. 122*, 627−633.
8. Thompson, S., Mayerl, F., Peoples, O. P., Masamune, S., Sinskey, A. J., and Walsh, C. T. (1989) *Biochemistry 28*, 5735−5742.
9. Shaw, W. V., and Leslie, A. G. (1991) *Annu. Rev. Biophys. Biophys. Chem. 20*, 363−386.
10. Tanner, K. G., Trievel, R. C., Kuo, M.-H., Howard, R. M., Berger, S. L., Allis, C. D., Marmorstein, R., and Denu, J. M. (1999) *J. Biol. Chem. 274*, 18157−18160.
11. Kleanthous, C., and Shaw, W. V. (1984) *Biochem. J. 223*, 211−220.
12. Ellis, J., Bagshaw, C. R., and Shaw, W. V. (1995) *Biochemistry 34*, 16852−16859.
13. Leslie, A. G. (1990) *J. Mol. Biol. 213*, 167−186.
14. Rojas, J. R., Trievel, R. C., Zhou, J., Mo, Y., Li, X., Berger, S. L., Allis, C. D., and Marmorstein, R. (1999) *Nature 401*, 93−98.
15. Leatherbarrow, R. J. (1990) *Trends Biochem. Sci., 15*, 455−458.
16. Cleland, W. W. (1982) *Methods Enzymol. 87*, 390−426.
17. Copeland, R. A. (2000) *Enzymes: A practical introduction to structure, mechanism, and data analysis*, 2nd ed., pp 241−248, Wiley-VCH, New York.
18. Bradford, M. M. (1976) *Anal. Biochem. 72*, 248−254.
19. Laemmli, U. K. (1970) *Nature 227*, 680−685.
20. Cleland, W. W. (1967) *Adv. Enzymol. 29*, 1−32.
21. Segel, I. H. (1975) in *Enzyme Kinetics*, pp 623−625, John Wiley & Sons, New York.
22. Brouillard, R., Dangles, O. (1994) Flavonoids and flower color in *The Flavonoids* (Harborne, J. B., Ed.) pp 565−599, Chapman & Hall/CRC, Washington, DC.
23. Lewendon, A., Murray, I. A., and Shaw, W. V. (1994) *Biochemistry 33*, 1944−1950.
24. Tanner, K. G., Langer, M. R., Kim, Y., and Denu, J. M. (2000) *J. Biol. Chem. 275*, 22048−22055.
25. Ollis, D. L., Cheah, E., Cygler, M., Dijkstra, B., Frolow, F., Franken, S. M., Harel, M., Remington, S. J., Silman, I., Schrag, J., Sussman, J. L., Verschueren, K. H. G., and Goldman, A. (1992) *Protein Eng. 5*, 197−211.
26. Yang, Q., Reinhard, K., Schiltz, E., and Matern, U. (1997) *Plant Mol. Biol. 35*, 777−789.
27. Grothe, T., Lenz, R., and Kutchan, T. M. (2001) *J. Biol. Chem. 276*, 30717−30723.
28. Walker, K., Schoendorf, A., and Croteau, R. (2000) *Arch. Biochem. Biophys. 374*, 371−380.
29. Walker, K., and Croteau, R. (2000) *Proc. Natl. Acad. Sci. U.S.A. 97*, 583−587.
30. Kimura, M., Kaneko, I., Komiyama, M., Takatsuki, A., Koshino, H., Yoneyama, K., and Yamaguchi, I. (1998) *J. Biol. Chem. 273*, 1654−1661.

BI020618G